# Detection of Linear Trends in Process Mean

H. M. FAHMY† and E. A. ELSAYED†*

**Abstract**

In this paper, we develop a process control approach to detect linear trends in the process mean. A statistic based on the deviation between the target mean and the expected mean of the process is used in the development of the new approach. The statistic is shown to have a Chi-square distribution. The approach is described and its performance is compared with Cumulative Sum (CUSUM), Exponentially Weighted Moving Average (EWMA), and Shewhart charts in detecting linear trends in the process mean. The results indicate that proposed approach is effective in detecting small to large trends. We also investigate the run length properties of the proposed approach under linear trends and compare its values with simulation results.

Finally, we analyze the performance of the proposed approach in detecting the time when a drift occurs in the process and compare it with CUSUM and EWMA estimators. The results show that the proposed approach is more effective in detecting drift time for moderate and large trends.

Keywords: Control charts; Linear trend; Change time detection

† Department of Industrial and Systems Engineering, Rutgers University, 96 Frelinghuysen Road, Piscataway, NJ 08854

* To whom correspondence should be addressed. email: elsayed@rci.rutgers.edu

## 1. Introduction

One of the most important problems in quality engineering is the detection of the shift in the process mean which occurs in different ways. The mean may increase/decrease suddenly and stays at the new value or it may increase/decrease gradually in a linear or a nonlinear fashion. The shift in the process mean may cause significant losses in product quality. Therefore, it is important to detect the shift as soon as it occurs and provide corrective actions in order to eliminate or minimize future occurrences of similar shifts. The traditional statistical quality control procedure is based on using standard Shewhart charts for detecting moderate to large process shifts while the Cumulative Sum (CUSUM) and the Exponentially Weighted Moving-Average (EWMA) charts are commonly used for small shift detection [Aerne *et al.*(1991), Montgomery (1997)].

Originally, the Shewhart control chart is used with only one rule to signal that there may be a problem with the process being monitored. The basic $\overline{X}$ - chart has a center line and three-sigma limits on either side of the center line. The chart signals an out of control condition if any observed $\overline{X}$ value falls beyond the three-sigma limits. Shewhart (1931) chooses three-sigma limits to prevent a large number of false alarms being signaled by the chart and ensures that 99.73% of the observations are within the normal process. It is well known, however, that this chart is insensitive to small shifts in the process mean. One method of overcoming this problem is to use the “supplementary run rules”. These rules are introduced by the Western Electric Company (1956). The power function of several combinations of these rules is derived by Wheeler (1983) and the rules are further investigated using a Markov chain approach by Champ and Woodall (1987). Davis and Woodall (1988) study the performance of the control chart trend rules under linear shift and concluded that it is ineffective in detecting a trend in the process mean. Their reasoning is that if the drift in process mean is large, then the observed points will almost certainly reach the control limits before the trend rule can generate a signal. If the drift is small, then the natural variation in the process makes the probability of five or six consecutive slopes having the same sign very small.

Based on a modification of the Markov chain method developed by Brook and Evans (1972), Bissell (1984) computes the performance of CUSUM charts under linear drifts in the process mean. However, the in-control average run lengths are not accurate, and the application of the results is limited due to rounding errors. Gan (1991, 1992, 1996) presents an accurate numerical method based on an integral equation for computing the average run length (ARL) of CUSUM and EWMA charts under linear trends, also a design procedure to determine the appropriate parameters of CUSUM and EWMA charts is provided. The results are accurate and comparable to those obtained using Monte Carlo simulation.

In this paper we propose a process control procedure to detect linear trends in the process mean based on a statistic which evaluates the deviation between the target mean and the expected mean of the process. Section 2 describes the process model for a process subject to linear trend in the process mean. The moving window procedure used to calculate the chart statistic is introduced in section 3 followed by the derivation of the chart statistic in section 4. The run length calculation for the proposed approach is presented in section 5. In section 6, we investigate the effect of the window size on the autocorrelation of the chart statistic. Simulation results are presented in section 7 for the performance of the proposed approach in detecting linear trends, designing the proposed control chart, and identifying the drift time.

## 2. Process Model

We consider a process in which individual observations are collected at fixed intervals of time. When the process is in the state of statistical control, observations are assumed to be normally and independently distributed from a normal distribution with a known mean $\mu_0$ and known variance $\sigma_0^2$. In the out-of-control state, the mean of the process is subjected to a linear trend. The amount of trend is $\beta\sigma_0 / unit\ time$ where $\beta$ is unknown. The observations collected from the out-of-control process follow a normal distribution at time $t$ (where $t$ is measured after the shift) with a mean $\mu_0 + \beta\sigma_0 t$ and variance $\sigma_0^2$. In other words,

$$y \sim N(\mu_0, \sigma_0^2) \qquad \text{in-control state}$$

$$y_t^* \sim N(\mu_0 + \beta\sigma_0 t, \sigma_0^2) \qquad \text{out-of-control state}$$

## 3. Window Procedure

A moving window of size $n$ is used to calculate the value of the proposed chart statistic along the data set. Hence, there is an overlap in the moving windows of $n-1$ observations.

The chart issues an out-of-control signal when the statistic reaches a certain threshold. Figure 1 shows the window procedure (window size=25) of a process with $\mu_0 = 10$ and $\sigma_0^2 = 1$ and its trend occurs at time $t$ = 50. The slope of the trend line is 0.25.

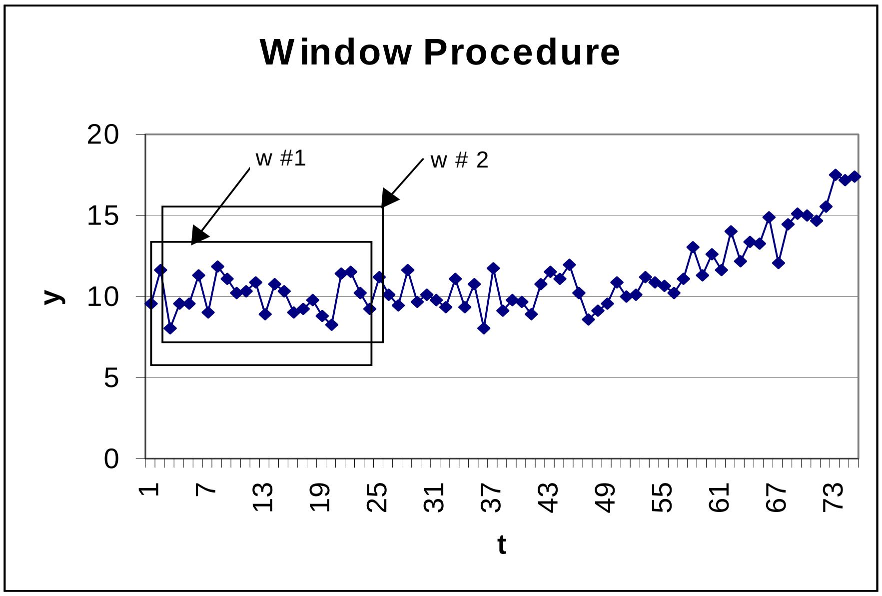


Figure 1. Window procedure for a process under linear trend

## 4. Derivation of the Proposed Statistic

The proposed control chart is developed to detect linear trends in the process mean. The chart uses a linear regression model to fit observations in a moving window of size $n$. The expected value for the process mean at the end of a window $j$ is defined as

$$\hat{\mu}_{nj} = \hat{\alpha}_j + \hat{\beta}_j t_n \qquad (1)$$

where $\hat{\alpha}_j$ and $\hat{\beta}_j$ are the least squares estimates for the linear regression model in window *j*.

The difference between target process mean and expected process mean at the end of window *j*; time $t_n$; is distributed as follows

$$\left(\mu - \hat{\mu}_{nj}\right) \sim N\left(0, \sigma^2\left(\frac{1}{n} + \frac{(t_n - \bar{t})^2}{S_{tt}}\right)\right) \tag{2}$$

where

$$S_{tt} = \sum_{i=1}^{n}\left(t_i - \bar{t}\right)^2$$

by normalizing (2), we obtain a standard normal distribution

$$\frac{(\mu - \hat{\mu}_{nj})}{\sqrt{\sigma^2\left(\frac{1}{n} + \frac{(t_n - \bar{t})^2}{S_{tt}}\right)}} \sim N(0,1) \tag{3}$$

Squaring the standard normal distribution in equation (3), a chi-square distribution with one degree of freedom is obtained.

$$\left[\frac{(\mu-\hat{\mu}_{nj})}{\sqrt{\sigma^2\left(\frac{1}{n}+\frac{(t_n-\bar{t})^2}{S_{tt}}\right)}}\right]^2 \sim \chi_1^2 \tag{4}$$

The upper control limit for the proposed chart is calculated as follows

$$P\left(\chi_1^2 > UCL / \mu_t = \mu_0\right) = \alpha \tag{5}$$

where $\alpha$ is the probability of type-I error.

Based on $\alpha = 0.0027$, the $UCL$=8.999 and the in-control $ARL = {}^1\!/_{\alpha} = {}^1\!/_{0.0027} = 370.370$.

## 5. Run Length Calculation under Linear Trend

We use Markov chain to calculate run length properties as discussed in Bissell (1984). In the case of linear trend, the distribution function, and hence the transition matrix, changes over time. The Markov chain transition matrix representation of Chi-square control chart is given below. In each case the row labels refer to states at observation $i-1$ and the column headings to states at observation $i$.

| | Clear | Signal |
|---|---|---|
| Clear | 1-$P_A$ | $P_A$ |
| Signal | 0 | 1 |

Figure 2. Transition matrix for Chi-square control chart

For an in-control process; $P_A$ is the probability of a violation of the action limit (*UCL*) for Chi-square distribution. For an out-control process with an accumulated shift in the mean equals to $\delta$ (in units of standard deviation); $P_A$ is the probability of a violation of the action limit for non-central Chi-square distribution with a non-central parameter equal to $\delta^2$.

$$P_A = P\left(\chi_1^2 > UCL\right), \qquad \text{for in-control}$$

$$P_A = P\left[\chi_1^2(\delta^2) > UCL\right], \qquad \text{for out-of-control}$$

For a non-homogeneous transition matrix, we use ${}^1P,\ {}^2P, etc.$ to represent the transition matrices deduced for the first, second, etc. observations. In general, the cumulative probability of a signal on or before the *ith* observation will be the (1,2)nd element in the product.

$${}^1P.{}^2P\ldots.{}^iP$$

Individual terms of the run length probability distribution are then obtained by subtraction of successive cumulative probabilities.

Consider a Chi-square control chart with $\alpha = 0.0027$, and linear trend $\beta\sigma = 1\sigma$. Then for the first observation (the process is in-control) the probability of violating the control limits is $P_A = 0.0027$ and the transition matrices are as follows

$${}^1P = \begin{pmatrix} 0.9973 & 0.0027 \\ 0 & 1 \end{pmatrix}$$

At the second observation, $1\sigma$ shift gives $P_A = 0.0227$

$$^{2}P = \begin{pmatrix} 0.9773 & 0.0227 \\ 0 & 1 \end{pmatrix}$$

$$^{1}P^{2}P = \begin{pmatrix} 0.9745 & 0.0255 \\ 0 & 1 \end{pmatrix}$$

The cumulative probability of a signal by observation 2 is 0.0255. Subtracting the (1,2)nd element of $^{1}P$ gives 0.0228 as the probability of the signaling at observation 2.

When the probability distribution has been evaluated, the average run length and the variance are computed as follows

$$ARL = \sum_{m=1}^{\infty} mP(L = m)$$

$$\mathrm{var}(RL) = \sum_{m=1}^{\infty} m^2 P(L = m) - ARL^2$$

The approximate values for the average and standard deviation of run length distribution for the Chi-square control procedure are shown in Table 1.

Table 1. Average run length and standard deviation of Chi-square control procedure

| $\beta\sigma$ | ARL | Standard deviation |
|---|---|---|
| 0 | 370.37 | 369.87 |
| 0.25 | 9.23 | 2.75 |
| 0.5 | 5.46 | 1.60 |
| 0.75 | 4.03 | 1.14 |
| 1.0 | 3.25 | 0.91 |
| 1.25 | 2.76 | 0.77 |
| 1.5 | 2.42 | 0.68 |
| 1.75 | 2.16 | 0.62 |
| 2.0 | 1.96 | 0.55 |

These values of the run length characteristics are obtained under the independence assumption of the chart statistic, which is inappropriate especially for large window sizes. The effect of the window size on the autocorrelation of the chart statistic is discussed in the following section.

**6. Effect of Window Size**

Since every two consecutive windows are overlapped by $n$-1 observations, we study the effect of window size on the independence among the values of the chart statistic. Simulation is used to generate a data set of 1000 observation and to apply the $\chi^2$ procedure with different window sizes for $n$ = 3,5,7, and 10. Then, autocorrelation coefficient is calculated at different lags. The results as shown in Table 2, indicate that the values of $\chi^2$ statistic are autocorrelated and the values of autocorrelation coefficient increase with the increase in window size. It is found that the autocorrelation coefficients for the window of size three are within the 95% acceptable limits. These results are validated by conducting three different tests for Randomness to test the hypothesis that the series is random (Number of runs above and below median, Number of times that the sequence goes up or down, the third test is Box-Pierce test which is based on the sum of squares of the first 24 autocorrelation coefficients). Only the $\chi^2$ chart with window of size three passes the Randomness tests above due to its smaller autocorrelation coefficient.

Table 2. Autocorrelation coefficients at different window sizes

| *n* | Lag | Autocorrelation | Std. Error | Lower 95% Limit | Upper 95% Limit |
|---|---|---|---|---|---|
| 3 | 1 | 0.041676 | 0.031654 | -0.06204 | 0.062042 |
| | 2 | 0.077507 | 0.031709 | -0.06215 | 0.062149 |
| | 3 | -0.02302 | 0.031899 | -0.06252 | 0.06252 |
| 5 | 1 | 0.287373 | 0.031686 | -0.0621 | 0.062104 |
| | 2 | 0.030135 | 0.034203 | -0.06704 | 0.067037 |
| | 3 | 0.012691 | 0.03423 | -0.06709 | 0.067089 |
| 7 | 1 | 0.449741 | 0.031718 | -0.06217 | 0.062166 |
| | 2 | 0.14369 | 0.03759 | -0.07368 | 0.073675 |
| | 3 | 0.024914 | 0.038139 | -0.07475 | 0.074751 |
| 10 | 1 | 0.54532 | 0.031766 | -0.06226 | 0.06226 |
| | 2 | 0.266994 | 0.040115 | -0.07862 | 0.078625 |
| | 3 | 0.125652 | 0.04187 | -0.08206 | 0.082064 |

## 7. Simulation Results

In this section, we analyze the performance of the proposed approach for the detection of linear trends and investigate its capability for the drift time identification under different linear trend rates. Monte Carlo simulation is used to perform these studies.

In all simulation studies, observations 1 to 50 are randomly generated from a normal distribution with mean 10.0 and standard deviation 1.0. Starting from observation 51, observations are randomly generated from a normal distribution with mean $10.0+(t-50)\beta$ (where $t>50$) and standard deviation 1.0 until the control chart issues a signal. This procedure is repeated 10,000 times for each value of $\beta$. This scenario is repeated with same randomly generated data to analyze the performance of the different control charts under different trend rates. Shewhart X-chart ($3\sigma$), CUSUM ($K$=0.25, $H$=8), and EWMA ($L$=2.7, $\lambda$=0.1) charts are compared with $\chi^2$ control chart with window sizes 3, 5 and 20. The parameters of these charts are set such that the control charts have almost equivalent performances based on the in-control average run length value 370.

The threshold values for the $\chi^2$ control chart with windows 3, 5 are set to 8.99, while the threshold value for the $\chi^2$ control chart with window 20 is set to 7.65, since its in-control ARL is significantly higher than other charts due to the large window size.

**7.1. Trend Detection Performance Analysis**

We simulate the process and calculate the ARL for the different control charts under different linear trend rates. The simulation results show that there is an agreement between the simulation results and the analytical results (Tables 3 and 4) for small size windows. Moreover, the in-control ARL increases with the increase of window size. Decreasing the window size of the $\chi^2$ control chart increases the ability to detect large trend rates while increasing the window size increases the ability to detect small trend rates.

It is also shown that the $\chi^2$ chart with different window sizes outperforms the CUSUM, EWMA and the Shewhart chart at the entire range of trend rates being studied. For example, $\chi^2$ chart with window size 20 outperforms other charts in the range from 0.1 to 0.5 while $\chi^2$ chart with window size 5 outperforms other charts in the range from 0.5 to

2.0. Window size 3 outperforms other charts in the range from 0.75 to 2.0. Thus, it can be seen that regardless of the magnitude of the trend, the proposed control chart procedure detects the trend in the process mean faster than the well-known charts being compared. Also, it should be noted that the autocorrelation between consecutive windows helps to increase the in-control ARL without delaying the out-of-control ARL performance.

Table 3. Simulation results for different trend rates using the $\chi^2$ charts

| | $\chi^2$ C*=8.99, *n**=3 | | $\chi^2$ C*=8.99, *n**=5 | | $\chi^2$ C*=7.65, *n**=20 | |
|---|---|---|---|---|---|---|
| $\beta\sigma$ | ARL | StdDev | ARL | StdDev | ARL | StdDev |
| 0 | 379.138 | 379.053 | 400.927 | 397.016 | 373.458 | 354.652 |
| 0.10 | 17.445 | 5.590 | 16.140 | 5.140 | 12.860 | 3.478 |
| 0.25 | 8.538 | 3.236 | 7.964 | 2.739 | 7.623 | 1.798 |
| 0.5 | 5.027 | 2.087 | 4.745 | 1.661 | 5.260 | 1.171 |
| 0.75 | 3.672 | 1.667 | 3.575 | 1.266 | 4.250 | 0.918 |
| 1.0 | 2.939 | 1.452 | 2.973 | 1.093 | 3.660 | 0.790 |
| 1.25 | 2.492 | 1.321 | 2.606 | 0.994 | 3.265 | 0.710 |
| 1.5 | 2.190 | 1.236 | 2.342 | 0.946 | 2.977 | 0.647 |
| 1.75 | 1.963 | 1.170 | 2.134 | 0.897 | 2.756 | 0.589 |
| 2.0 | 1.816 | 1.121 | 1.972 | 0.839 | 2.579 | 0.572 |

C: Threshold value for the $\chi^2$ chart
*n*: Window size

Table 4. Simulation results for CUSUM, EWMA, and X-Chart charts under linear trends

| | CUSUM *H*=8, *K*=0.25 | | EWMA *L*=2.7, $\lambda$ =0.1 | | X-Chart 3 $\sigma$ | |
|---|---|---|---|---|---|---|
| $\beta\sigma$ | ARL | StdDev | ARL | StdDev | ARL | StdDev |
| 0 | 368.333 | 354.861 | 365.749 | 359.791 | 372.789 | 374.847 |
| 0.10 | 13.986 | 2.644 | 12.971 | 2.929 | 18.476 | 5.686 |
| 0.25 | 8.560 | 1.385 | 7.738 | 1.508 | 9.275 | 2.687 |
| 0.5 | 5.946 | 0.853 | 5.312 | 0.931 | 5.512 | 1.547 |
| 0.75 | 4.827 | 0.661 | 4.279 | 0.726 | 4.050 | 1.118 |
| 1.0 | 4.156 | 0.563 | 3.680 | 0.613 | 3.261 | 0.899 |
| 1.25 | 3.729 | 0.497 | 3.271 | 0.554 | 2.763 | 0.760 |
| 1.5 | 3.372 | 0.501 | 2.979 | 0.464 | 2.426 | 0.667 |
| 1.75 | 3.102 | 0.374 | 2.782 | 0.451 | 2.171 | 0.610 |
| 2.0 | 2.950 | 0.300 | 2.598 | 0.495 | 1.974 | 0.546 |

## 7.2. Design of $\chi^2$ Control Chart

Additional simulation runs are conducted to establish a relationship between the in-control ARL and the threshold value ($C$) of the $\chi^2$ control chart with window size $n$=3, 5, and 20 using regression analysis. The in-control ARLs ($ARL_0$) are estimated at intervals of 0.25 in the range $5 \le C \le 10$ with 10,000 simulation runs. Box-Cox power transformation method (see, Draper and Smith (1981)) is used to minimize the mean squared error of the linear regression model between the transformed response ($ARL_0$) and the threshold value ($C$).

Box and Cox (1964) propose a parametric family of power transformations:

$$W = \begin{cases} \left(Y^{\lambda} - 1\right)/\lambda, & \text{for } \lambda \neq 0 \\ \ln Y, & \text{for } \lambda = 0 \end{cases}$$

This continuous family depends on a single parameter $\lambda$. We can use the data to estimate this parameter, as well as the vector of parameters $\beta$ in the model to be fitted,

$$W = X\beta + \varepsilon$$

Where $W$ is the Box-Cox transformation of the response variable $Y$ and $X$ is the regressor variable.

The equation of the fitted model for the $\chi^2$ control chart with window size $n$=3 is

$$BoxCox\left(ARL_0\right) = 160.412 + 91.121C$$

Where

$$BoxCox\left(ARL_0\right) = 1 + \frac{ARL_0^{0.00496} - 1}{0.00496 \times 166.768^{-0.99503}}$$

Thus, to obtain a value of *C* for the $\chi^2$ control chart for a given $ARL_0$, an approximate value of *C* would be

$$\hat{C} = \frac{1}{91.1216}\left(-159.412 + \frac{ARL_0^{0.00496} - 1}{0.00496 \times 166.768^{-0.99503}}\right)$$

The R-Squared statistic of this model indicates that the model as fitted explains 99.9983% of the variability in $ARL_0$. The correlation coefficient equals 0.999991, indicating a relatively strong relationship between the variables. Figure 2 shows the relationship between the observed and predicted values of the $ARL_0$ from the regression model.

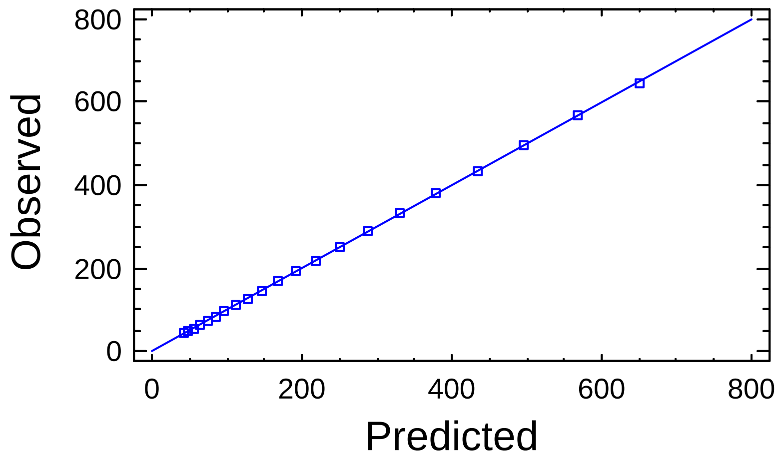


Figure 2. Observed and predicted values of the $\text{ARL}_0$ for $\chi^2$ control chart with $n$=3

For the $\chi^2$ control chart with window size $n$=5, the regression model that describes the relationship between $\text{ARL}_0$ and $C$ is

$$BoxCox(ARL_0) = 283.2 + 95.1989C$$

where

$$BoxCox(ARL_0) = 1 + \frac{ARL_0^{-0.01562} - 1}{-0.01562 \times 183.593^{-1.01562}}$$

The $C$ value of the $\chi^2$ control chart for a given $\text{ARL}_0$ can be approximated by

$$\hat{C} = \frac{1}{95.1989}\left(-282.2 + \frac{ARL_0^{-0.01562} - 1}{-0.01562 \times 183.593^{-1.01562}}\right)$$

The R-Squared statistic of the regression model indicates that the model as fitted explains 99.9919% of the variability in $ARL_0$. The correlation coefficient equals 0.99996, indicating a relatively strong relationship between the variables. The relationship between the observed and predicted values of $ARL_0$ is shown in figure 3.

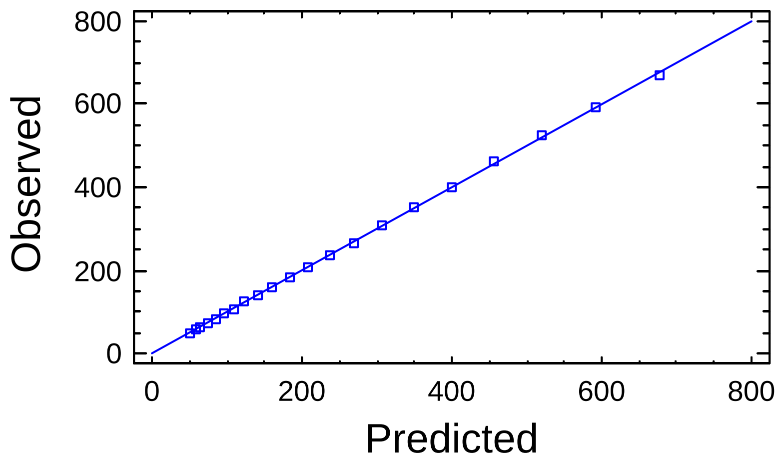


Figure 3. Observed and predicted values of the $ARL_0$ for $\chi^2$ control chart with $n$=5

Finally, for the $\chi^2$ control chart with window size $n$=20, the relationship between $ARL_0$ and $C$ is described by the following regression model

$$BoxCox(ARL_0) = 714.65 + 157.276C$$

where

$$BoxCox(ARL_0) = 1 + \frac{ARL_0^{0.02376} - 1}{0.02376 \times 346.419^{-0.97623}}$$

The expression of the $C$ value for a given $ARL_0$ can be approximated by

$$\hat{C} = \frac{1}{157.276}\left( -713.65 + \frac{ARL_0^{0.02376} - 1}{0.02376 \times 346.419^{-0.97623}} \right)$$

The R-Squared statistic and the correlation coefficient of the regression model are 99.9607% and 0.999804 respectively, indicating a relatively strong relationship between the variables. The relationship between the observed and predicted values of $ARL_0$ for a window size 20 is shown in figure 4.

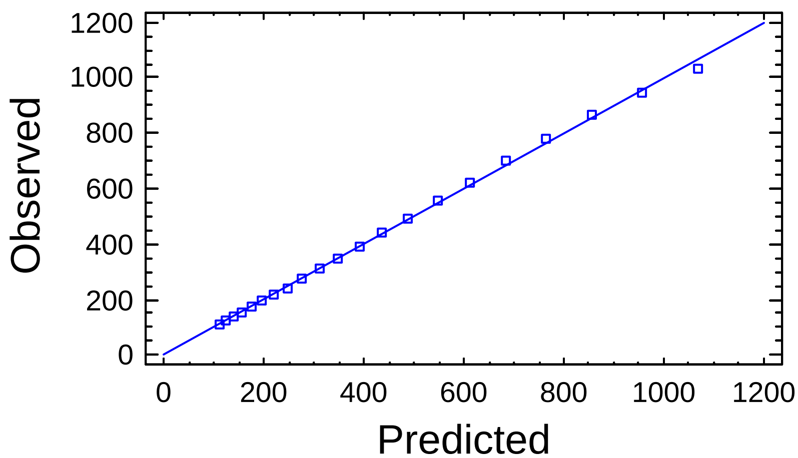


Figure 4. Observed and predicted values of the $ARL_0$ for $\chi^2$ control chart with $n$=20

To check the performance of the regression models for predicting the threshold value $\hat{C}$ of the $\chi^2$ control chart at $n$=3, 5, and 20, we calculate $\hat{C}$ at different values of $ARL_0$ ($ARL_0$=100, 250, 350, and 500) and then estimate the actual $ARL_0$ by simulation. The results of table 5 indicate that Box-Cox power transformation method can accurately approximate the $ARL_0$ of the $\chi^2$ control chart.

Table 5. Estimation of the $ARL_0$ by using Box-Cox power transformation method

| | | 100 | 250 | 350 | 500 |
|---|---|---|---|---|---|
| $n$=3 | $\hat{C}$ | 6.556 | 8.231 | 8.848 | 9.504 |
| | $ARL_0$ | 99.261 | 248.705 | 349.803 | 498.787 |
| $n$=5 | $\hat{C}$ | 6.331 | 8.102 | 8.746 | 9.425 |
| | $ARL_0$ | 100.447 | 246.620 | 353.017 | 505.068 |
| $n$=20 | $\hat{C}$ | 4.797 | 6.779 | 7.518 | 8.307 |
| | $ARL_0$ | 102.519 | 246.450 | 350.620 | 507.764 |

## 7. 3. Time Detection Performance Analysis

Time $\tau$ at which a trend starts can be estimated by applying the proposed approach since the value of the proposed statistic increases monotonically when a trend occurs. We compare the performance of the proposed method with CUSUM and EWMA estimators.

### 7.3.1. Chi-square Change Point Estimation Procedure

a) $\chi^2$ control chart issues an out-of-control signal when the chart value at the *Tth* window; $\left[\chi^2\right]_T$; exceeds the *UCL*

b) The time of the drift occurrence is identified by counting the number of consecutive periods since the chart values are monotonically increasing

$$\hat{\tau}_{\chi^2} = \left\{ t : \left[\chi^2\right]_t \geq \left[\chi^2\right]_{t+1},\ \left[\chi^2\right]_i < \left[\chi^2\right]_{i+1}\ \left(i = t+1, \ldots .T-1\right),\ \left[\chi^2\right]_T \geq UCL \right\} \tag{6}$$

A $\chi^2$ control chart with *UCL*=7.65 and window size 20 is used to apply the $\chi^2$ estimator in the10,000 simulation runs.

### 7.3.2. CUSUM Change Point Estimation Procedure

The CUSUM estimator procedure proposed by Page (1954) is summarized for a CUSUM chart with parameters *K* and *H* as follows

a) CUSUM statistics are

$$C_i^+ = \max\left[0, y_t - (\mu_0 + K) + C_{i-1}^+\right] \tag{7}$$

$$C_i^- = \max\left[0, (\mu_0 - K) - y_t + C_{i-1}^-\right] \tag{8}$$

where the starting values are $C_0^+ = C_0^- = 0$

b) CUSUM chart issues an out-of-control signal when $C_i^+$ or $C_i^-$ exceeds the control limit *H*

b) If $C_i^+ \geq H$, the time of the drift occurrence is identified by counting the number of consecutive periods since $C_i^+$ is greater than zero. The same procedure is used when $C_i^- \geq H$. The change point estimate using CUSUM chart to identify the change point $\tau$ can be expressed as

$$\hat{\tau}_{CUSUM} = \left\{t : C_t^{\pm} \leq 0, 0 < C_i^{\pm} < H \left(i = t+1, \ldots .T-1\right), C_T^{\pm} \geq H\right\} \tag{9}$$

A CUSUM control chart with parameters $K$=0.25, and $H$=8 is used in simulating 10,000 runs.

### 7.3.3. EWMA Change Point Estimation Procedure

A similar approach to the CUSUM estimator is proposed by Nishina (1992) to use EWMA control charts to identify the change point in a process. The EWMA estimator is summarized for an EWMA chart with parameters $\lambda$ and $L$ as follows

a) EWMA statistics $E_t$ at time $t$ is defined as

$$E_t = \lambda\, y_t + (1-\lambda)E_{t-1} \tag{10}$$

where $0 < \lambda \leq 1$ and $E_0 = \mu_0$

b) EWMA chart issues an out-of-control signal when $E_t$ exceeds the control limits

$$UCL_t = \mu_0 + L\sigma\sqrt{\frac{\lambda}{(2-\lambda)}\left[1-(1-\lambda)^{2t}\right]} \tag{11}$$

$$LCL_t = \mu_0 - L\sigma\sqrt{\frac{\lambda}{(2-\lambda)}\left[1-(1-\lambda)^{2t}\right]} \tag{12}$$

c) If $E_t \geq UCL_t$, the time of the shift occurrence is identified by counting the number of consecutive periods since $E_t$ exceeds the standard mean $\mu_0$. The EWMA estimator for the change point $\tau$ can be expressed as

$$\hat{\tau}_{EWMA} = \{t : E_t \leq \mu_0,\, \mu_0 < E_i < UCL_i \ (i = t+1, \ldots, T-1),\, E_T \geq UCL_T\} \qquad (13)$$

An EWMA control chart with parameters $L$=2.7, and $\lambda$ =0.1 is used to apply the CUSUM estimator in the10,000 simulation runs.

The simulation results for the different drift time estimators are shown in tables 6 and 7. Table 6 shows the expected value of the deviation $d$ and its standard error for different trend rates. The deviation $d$ is the difference between the estimate of drift time $\hat{\tau}$ and the actual drift time $(\tau = 50)$; i.e., $d = \hat{\tau} - \tau$.

Table 6. Simulation results for the estimates of drift time

| $\beta$ | $\chi^2$ Estimator | | CUSUM Estimator | | EWMA Estimator | |
|---|---|---|---|---|---|---|
| | $E(d)$ | Std. error | $E(d)$ | Std. error | $E(d)$ | Std. error |
| 0.1 | 9.46 | 0.040 | -2.70 | 0.110 | -0.63 | 0.101 |
| 0.2 | 4.92 | 0.027 | -4.54 | 0.105 | -2.53 | 0.097 |
| 0.3 | 3.15 | 0.021 | -5.28 | 0.104 | -3.32 | 0.095 |
| 0.4 | 2.21 | 0.018 | -5.68 | 0.103 | -3.72 | 0.094 |
| 0.5 | 1.64 | 0.016 | -5.94 | 0.103 | -3.99 | 0.094 |
| 0.6 | 1.25 | 0.015 | -6.10 | 0.102 | -4.18 | 0.093 |
| 0.7 | 0.98 | 0.014 | -6.22 | 0.102 | -4.32 | 0.093 |
| 0.8 | 0.78 | 0.013 | -6.31 | 0.102 | -4.42 | 0.093 |
| 0.9 | 0.63 | 0.013 | -6.40 | 0.102 | -4.51 | 0.092 |
| 1.0 | 0.50 | 0.012 | -6.46 | 0.102 | -4.59 | 0.092 |

The results show that on average the $\chi^2$ estimator is more efficient than CUSUM and EWMA estimators in detecting the drift time for trend rates greater than 0.2. Also, it can be seen that the standard error of the proposed estimator is significantly smaller than the standard error of the other estimators.

The estimated probability of drift time detection within *n* observations from the actual drift time is shown in table 7, where $\hat{p}(|\hat{\tau}-\tau| \le n)$ is the estimated probability that the absolute difference between $\hat{\tau}$ and $\tau$ is less than or equal *n*.

Table 7. Estimated probability of detecting the actual drift time

| $\beta$ | | 0.1 | 0.2 | 0.3 | 0.4 | 0.5 | 0.6 | 0.7 | 0.8 | 0.9 | 1.0 |
|---|---|---|---|---|---|---|---|---|---|---|---|
| $\hat{p}(\hat{\tau}=\tau)$ | $\chi^2$ | 0.008 | 0.027 | 0.055 | 0.093 | 0.129 | 0.165 | 0.194 | 0.224 | 0.247 | 0.265 |
| | CUSUM | 0.067 | 0.102 | 0.130 | 0.152 | 0.170 | 0.190 | 0.204 | 0.218 | 0.229 | 0.241 |
| | EWMA | 0.048 | 0.068 | 0.084 | 0.101 | 0.114 | 0.127 | 0.144 | 0.159 | 0.173 | 0.187 |
| $\hat{p}(\lvert\hat{\tau}-\tau\rvert \le 1)$ | $\chi^2$ | 0.025 | 0.088 | 0.187 | 0.300 | 0.405 | 0.487 | 0.554 | 0.613 | 0.657 | 0.694 |
| | CUSUM | 0.184 | 0.273 | 0.336 | 0.377 | 0.407 | 0.425 | 0.435 | 0.440 | 0.444 | 0.444 |
| | EWMA | 0.136 | 0.199 | 0.250 | 0.297 | 0.336 | 0.372 | 0.405 | 0.432 | 0.461 | 0.484 |
| $\hat{p}(\lvert\hat{\tau}-\tau\rvert \le 2)$ | $\chi^2$ | 0.051 | 0.177 | 0.365 | 0.548 | 0.688 | 0.792 | 0.866 | 0.914 | 0.947 | 0.970 |
| | CUSUM | 0.305 | 0.431 | 0.500 | 0.530 | 0.541 | 0.543 | 0.541 | 0.537 | 0.533 | 0.530 |
| | EWMA | 0.231 | 0.339 | 0.422 | 0.490 | 0.539 | 0.573 | 0.600 | 0.614 | 0.624 | 0.628 |
| $\hat{p}(\lvert\hat{\tau}-\tau\rvert \le 3)$ | $\chi^2$ | 0.075 | 0.288 | 0.556 | 0.761 | 0.884 | 0.950 | 0.979 | 0.993 | 0.998 | 1.000 |
| | CUSUM | 0.418 | 0.552 | 0.600 | 0.607 | 0.604 | 0.600 | 0.595 | 0.591 | 0.587 | 0.585 |
| | EWMA | 0.331 | 0.483 | 0.582 | 0.634 | 0.661 | 0.672 | 0.676 | 0.676 | 0.675 | 0.674 |
| $\hat{p}(\lvert\hat{\tau}-\tau\rvert \le 4)$ | $\chi^2$ | 0.112 | 0.436 | 0.743 | 0.905 | 0.973 | 0.994 | 0.999 | 1.000 | 1.000 | 1.000 |
| | CUSUM | 0.523 | 0.646 | 0.665 | 0.659 | 0.651 | 0.647 | 0.643 | 0.640 | 0.637 | 0.634 |
| | EWMA | 0.437 | 0.614 | 0.686 | 0.711 | 0.714 | 0.712 | 0.710 | 0.708 | 0.707 | 0.706 |
| $\hat{p}(\lvert\hat{\tau}-\tau\rvert \le 5)$ | $\chi^2$ | 0.160 | 0.588 | 0.874 | 0.971 | 0.995 | 0.999 | 1.000 | 1.000 | 1.000 | 1.000 |
| | CUSUM | 0.610 | 0.703 | 0.702 | 0.693 | 0.686 | 0.682 | 0.678 | 0.676 | 0.673 | 0.671 |
| | EWMA | 0.536 | 0.701 | 0.745 | 0.745 | 0.741 | 0.737 | 0.735 | 0.733 | 0.732 | 0.731 |
| $\hat{p}(\lvert\hat{\tau}-\tau\rvert \le 6)$ | $\chi^2$ | 0.224 | 0.720 | 0.947 | 0.994 | | | | | | |
| | CUSUM | 0.679 | 0.738 | 0.728 | 0.719 | | | | | | |
| | EWMA | 0.628 | 0.764 | 0.773 | 0.768 | | | | | | |
| $\hat{p}(\lvert\hat{\tau}-\tau\rvert \le 7)$ | $\chi^2$ | 0.298 | 0.829 | 0.986 | 0.999 | | | | | | |
| | CUSUM | 0.730 | 0.764 | 0.752 | 0.743 | | | | | | |
| | EWMA | 0.704 | 0.800 | 0.796 | 0.790 | | | | | | |
| $\hat{p}(\lvert\hat{\tau}-\tau\rvert \le 8)$ | $\chi^2$ | 0.389 | 0.908 | 0.997 | 1.000 | | | | | | |
| | CUSUM | 0.772 | 0.785 | 0.774 | 0.767 | | | | | | |
| | EWMA | 0.765 | 0.822 | 0.813 | 0.808 | | | | | | |
| $\hat{p}(\lvert\hat{\tau}-\tau\rvert \le 9)$ | $\chi^2$ | 0.489 | 0.963 | 1.000 | 1.000 | | | | | | |
| | CUSUM | 0.805 | 0.802 | 0.792 | 0.785 | | | | | | |
| | EWMA | 0.813 | 0.837 | 0.828 | 0.823 | | | | | | |
| $\hat{p}(\lvert\hat{\tau}-\tau\rvert \le 10)$ | $\chi^2$ | 0.591 | 0.988 | 1.000 | 1.000 | | | | | | |
| | CUSUM | 0.827 | 0.818 | 0.809 | 0.803 | | | | | | |
| | EWMA | 0.846 | 0.850 | 0.841 | 0.837 | | | | | | |

The results indicate that the probability of detection of the proposed estimator significantly increases with the increase in the number of observations *n*. As a result, the proposed estimator is capable of detecting the true drift time within 5 observations with probability greater than 0.97 for $\beta > 0.4$ which is approximately 30% higher than the other estimators.

## 8. Conclusions

The performance of the proposed chart for detecting linear trends in process mean is investigated and compared with CUSUM, EWMA, and Shewhart charts. The comparisons reveal the effectiveness and the capability of Chi-square chart to deal with a wide range of trend magnitudes. Simulations are used to study the applicability of the new chart for detecting drift time in a process subject to a linear trend in process mean. Also, the ARL properties of Chi-square chart are investigated analytically using Markov chain approach.

## References

AERNE, A., CHAMP, C. W. and RIGDON, S. E., 1991, Evaluation of control charts under linear trend. *Communications in Statistics-Theory and Methods,* 20, 3341-3349.

BISSELL, A. F., 1984, The performance of control charts and Cusums under linear trend. *Applied Statistics,* 33, 145-151.

BOX, G. E. P. and D. R. COX, 1964, An analysis of transformations (with discussion). *Journal of Royal Statistical Society, Series B,* 26, 211-246.

BROOK, D. and EVANS, D. A., 1972, an approach to the probability distribution of cusum run length. *Biometrika*, 59, 539-549.

CHAMP, C. W. and WOODALL, W. H., 1987, Exact results for Shewhart control charts with supplementary run rules. *Technometrics,* 29, 393-399.

DAVIS, R. B. and WOODALL, W. H., 1988, Performance of the control chart trend rule under linear shift. *Journal of Quality and Technology*, 20, 260-262.

DRAPER, N. R. and SMITH, H., 1981, *Applied Regression Analysis* (New York, NY: 2nd ed. John Wiley & Sons).

GAN, F. F., 1991, EWMA control chart under linear drift. *Journal of Statistical Computation and Simulation,* 38, 181-200.

GAN, F. F., 1992, CUSUM control charts under linear drift. *The Statistician,* 41,71-84.

GAN, F. F., 1996, Average run lengths for cumulative sum control charts under linear trend. *Applied Statistics*, 45, 505-526.

MONTGOMERY, D. C., 1997, *Introduction to Statistical Quality Control* (New York, NY: 3rd ed. John Wiley & Sons).

NISHINA, K., 1992, A comparison of control charts from the viewpoint of change-point estimation. *Quality and Reliability Engineering International*, 8, 537-541.

PAGE, E. S., 1954, Continuous inspection schemes. *Biometrics*, 41, 100-115.

SHEWHART, W. A., 1931, *Economic Control of Quality of Manufactured Product* (New York, NY: D. Van Nostrand).

WESTERN ELECTRIC COMPANY, 1956, *Statistical Quality Control Handbook* (Chicago, IL: American Telephone and Telegraph Company).

WHEELER, D. J., 1983, Detecting a shift in process average: tables of the power function for $\bar{x}$ charts. *Journal of Quality and Technology*, 15, 155-170.